analytical chemistry

Article

pubs.acs.org/ac

Near Infrared Surface Plasmon Resonance Phase Imaging and Nanoparticle-Enhanced Surface Plasmon Resonance Phase Imaging for Ultrasensitive Protein and DNA Biosensing with Oligonucleotide and Aptamer Microarrays

Wen-Juan Zhou, Aaron R. Halpern, Ting H. Seefeld, and Robert M. Corn*

Department of Chemistry, University of California-Irvine, Irvine, California 92697, United States

Supporting Information

ABSTRACT: The techniques of surface plasmon resonance-phase imaging (SPR-PI) and nanoparticle-enhanced SPR-PI have been implemented for the multiplexed bioaffinity detection of proteins and nucleic acids. The SPR-PI experiments utilized a near-infrared 860 nm light emitting diode (LED) light source and a wedge depolarizer to create a phase grating on a four-element single-stranded DNA (ssDNA) microarray; bioaffinity adsorption onto the various microarray elements was detected via multiplexed real time phase shift measurements. In a first set of demonstration experiments, an ssDNA aptamer microarray was used to directly detect thrombin at concentrations down to 100 pM with SPR-PI. Two different ssDNA aptamers were used in these experiments with two different Langmuir adsorption coefficients, $K_{A1} = 4.4 \times 10^8\ M^{-1}$ and $K_{A2} = 1.2 \times 10^8\ M^{-1}$. At concentrations below 1 nM, the equilibrium phase shifts observed upon thrombin adsorption vary linearly with concentration with a slope that is proportional to the appropriate Langmuir adsorption coefficient. The observed detection limit of 100 pM is approximately 20 times more sensitive than that observed previously with SPRI. In a second set of experiments, two short ssDNA oligonucleotides (38mers) were simultaneously detected at concentrations down to 25 fM using a three-sequence hybridization format that employed 120 nm DNA-modified silica nanoparticles to enhance the SPR-PI signal. In this first demonstration of nanoparticle-enhanced SPR-PI, the adsorbed silica nanoparticles provided a greatly enhanced phase shift upon bioaffinity adsorption due to a large increase in the real component of the interfacial refractive index from the adsorbed nanoparticle. As in the case of SPR-PI, the detection limit of 25 fM for nanoparticle-enhanced SPR-PI is approximately 20 times more sensitive than that observed previously with nanoparticle-enhanced SPRI.

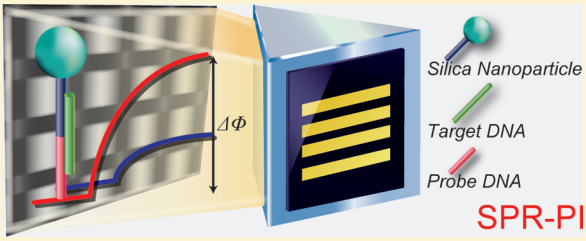

The multiplexed detection of biomolecules by the process of bioaffinity adsorption onto protein and DNA microarrays has become a mainstay tool for biological researchers throughout the world.[1,2] Surface plasmon resonance imaging (SPRI) is a well-established methodology for detecting the adsorption of proteins and nucleic acids onto DNA,[3] RNA,[4] peptide,[5] protein,[6] and carbohydrate microarrays.[7] For a typical biological target molecule with a molecular weight of 10 kDa or higher and bioaffinity Langmuir adsorption constant K_{ads} of $10^7\ M^{-1}$ or greater (corresponding to a K_d of 100 nM or less), SPRI typically has sufficient sensitivity to detect bioaffinity adsorption onto chemically modified gold thin films at concentrations of 1 nM or higher.[8]

In a recent paper, we have described a multiplexed implementation of a related technique, SPR phase imaging (SPR-PI), that can potentially serve as a more sensitive replacement for SPRI.[9] SPR-PI measures the phase shift of the p-polarized reflected light that occurs when surface plasmon polaritons (SPPs) are injected onto a gold thin film surface in the Kretschmann coupling configuration. By monitoring changes in the phase shift from light incident at a fixed angle, adsorption to the interface can be measured.[10−13] In our previous paper, a phase grating at 633 nm was created on a gold thin film perpendicular to a line microarray of sensing elements. This phase grating was converted to an intensity grating image on a CCD detector that could be used to quantitatively measure the phase shift from each of the line microarray elements in order to monitor multiple bioaffinity adsorption processes simultaneously. The results of measurements on full alkanethiol monolayers and fully hybridized DNA monolayers suggested that SPR-PI could in principle be between 1 to 2 orders of magnitude more sensitive than SPRI.

In this paper, we demonstrate that SPR-PI can be used for bioaffinity adsorption measurements at picomolar and even femtomolar target biomolecule concentrations. For these experiments, we have fabricated a new SPR-PI apparatus that uses a near-infrared LED light source at 860 nm and a four element DNA microarray that is spatially matched to a 20 μL microfluidic chamber (see Figure 1). In a first example, a single stranded DNA (ssDNA) microarray that contains two different

Received: October 30, 2011
Accepted: November 29, 2011
Published: November 29, 2011

   dx.doi.org/10.1021/ac202863k | *Anal. Chem.* 2012, 84, 440−445

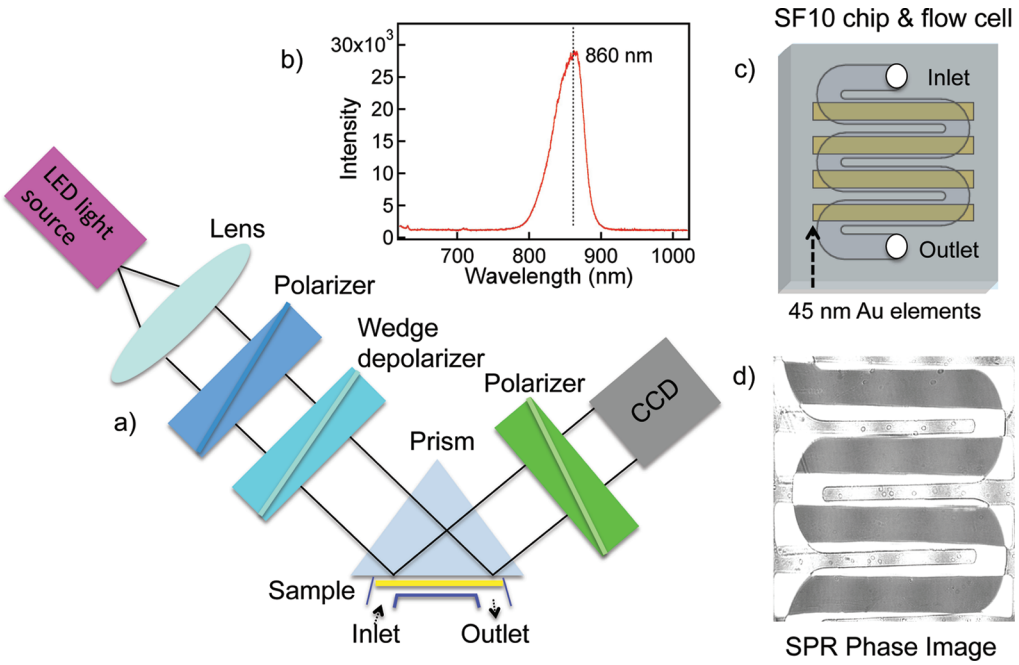

Figure 1. (a) Schematic diagram of the near infrared SPR-PI optical setup. (b) LED light source emission spectrum. (c) Schematic layout of gold strips and flow cell. (d) Sample SPR phase image with interference fringes created on four microarray elements.

Table 1. DNA and Aptamer Sequences Used in the SPR-PI and Nanoparticle-Enhanced SPR-PI Measurements

A1: 5′-NH_2-TTTTTTTTTTTTTTTTGGTTGGTGTGGTTGG-3′
A2: 5′-AGTCCGTGGTAGGGCAGGTTGGGGTGACTTTTTTTTTTTTTTTT-NH_2-3′
T1: 5′-$(T)_{16}$-TTA ACA CTT GAG GCT AAC ACT T-3′
T2: 5′-$(T)_{19}$-GCT GAT CGA CGA ATA CAT T-3′
S1: 5′-NH_2-$(CH_2)_{12}$-AAG TGT TAG CCT CAA GTG TT-3′
S2: 5′-NH_2-$(CH_2)_{12}$-AAT GTA TTC GTC GAT CAG CA-3′
D_{NP}: 5′-ACA CAT AAG ATC CAA C-NH_2-3′
Control-1: 5′-NH_2-AAT GTA TTC GTC GAT GTG GA-3′
Control-2: 5′-NH_2-ACA CAT AAG ATC CAA C-3′

ssDNA aptamers is used for the direct detection of bovine thrombin at concentrations down to 100 pM with SPR-PI. In a second set of experiments, two ssDNA target oligonucleotides (38mers) are simultaneously detected by adsorption onto ssDNA microarrays at concentrations down to 25 fM using a three-sequence hybridization format that employed 120 nm DNA-modified silica nanoparticles (SiNPs) to enhance the SPR-PI signal. In this first application of "nanoparticle-enhanced SPRI-PI", SiNPs that only have a real refractive index were chosen over gold or silver nanoparticles because their optical effect on the phase grating measurements is straightforward and easy to model.

EXPERIMENTAL CONSIDERATIONS

Materials. 11-Amino-1-undecanethiol hydrochloride (MUAM, Dojindo), poly-L-glutamic acid sodium salt (pGlu, MW = 3−15 kDa, Sigma), 1-ethyl-3-(3-(dimethylamino)-propyl)carbodiimide hydrochloride (EDC; Pierce), *N*-hydroxysulfosuccinimide (NHSS; Pierce), silica nanoparticles (mean size 120 nm, Bangs Laboratories), 3-aminopropyltrimethoxysilane (APTMS, 97%, Aldrich), and ethanol (Gold Shield) were used as received. Bovine thrombin was purchased from Haematologic Technologies Inc. DNA oligonucleotides were obtained from Integrated DNA Technologies (IDT) (sequences are listed in Table 1) and used as received. A PBS buffer (10 mM NaH_2PO_4, 2.7 mM KCl, 0.137 M NaCl, pH = 7.4) was used for all DNA array fabrication, DNA/DNA hybridization, and aptamer/protein binding measurements.

Surface Plasmon Resonance Phase Imaging (SPR-PI) Measurements. A schematic diagram of the SPR-PI setup is shown in Figure 1a and is described in detail in our previous report.[9] In this work, the light source is a near-IR LED light source with a maximum emission at 860 nm (OSRAM, SFH 4350) as shown in Figure 1b. The light is collimated with a lens, then polarized, and passed through the wedge depolarizer (Special Optics, 80-1015-633) where the periodic phase grating is created. It then interacts with the microarray coupled on the back of an SF10 equilateral prism. The reflected light passes through the second linear polarizer and is collected by a CCD camera (QICAM, Qimaging) as an intensity pattern. The microarray consists of four gold thin film strips (45 nm × 1 mm × 10 mm) evaporated onto SF10 slides (Schott Glass, 18 × 18 mm^2) through a shadow mask following a 1 nm chromium adhesion layer with a Denton DV-502A metal evaporator. Prior to evaporation, the entire glass surface is made hydrophobic for ease of spotting. This procedure involves activating the slide in an O_2 plasma, dipping in Sigmacote (Sigma), and rinsing with hexane, ethanol, and water to remove any residue. The slide is coupled to a 60° SF10 prism with index matching oil (Cargille). The flow-cell and SF10 glass substrate assembly form a fluidic

dx.doi.org/10.1021/ac202863k | *Anal. Chem.* 2012, 84, 440−445

channel as shown schematically in Figure 1c. The SPR phase images are continuously collected every 50 ms and averaged over a 3 s interval (Figure 1d). The dark areas correspond to the gold surface exposed to liquid at the SPR angle, and the U-shape bright areas are total internal reflection (TIR) off the glass. The positions of the interference fringes are monitored and the movement of the fringes is converted to phase shift ($\Delta\phi$) (Figure 2). The $\Delta\phi$ is calculated from the image using the mathematical methods described in our previous paper.[9]

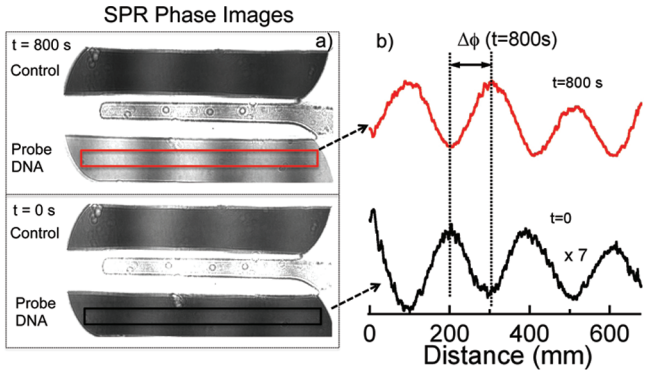

Figure 2. (a) Sample SPR phase images of control DNA and probe DNA elements at t = 0 s and at t = 800 s after flowing a solution of cDNA-modified nanoparticles. (b) The movement of the fringes after adsorption hybridization of DNA-modified nanoparticles is converted to phase shift ($\Delta\phi$).

DNA/Aptamer Microarray Fabrication. DNA/aptamer microarrays were fabricated using a three-step process as described previously.[14,15] The gold strip coated slides were immersed in a 1 mM ethanolic MUAM solution overnight. A pGlu monolayer was then formed by electrostatic adsorption onto the amino-terminated MUAM using a 2 mg/mL pGlu solution in PBS buffer for 1 h. Finally, each gold strip was exposed to a 250 μM amino-modified ssDNA solution in PBS buffer that contained 75 mM EDC and 15 mM NHSS for 4 h to covalently link the MUAM monolayer and amino-modified ssDNA to form the ssDNA microarray elements.

Synthesis of ssDNA-Modified SiNPs. The ssDNA-modified SiNPs were synthesized according to our previous report[15] with slight procedural adjustments. The process contains three steps. (1) Amino-functionalization of SiNPs. A solution of SiNPs (120 nm average diameter, 0.05 mL), APTMS (4 μL), and ethanol (8 mL) were gently stirred at room temperature for 24 h, centrifuged, and washed three times at 5000 rpm for 10 min then redispersed in 1 mL of water. (2) pGlu modification of SiNPs. The SiNPs were modified by reaction overnight in 1 mL of a solution containing 2.5 mg of pGlu adjusted to a pH of 6 by HCl. Excess pGlu was removed by discarding the supernatant after centrifugation, and the nanoparticles were redispersed in 1 mL water. (3) ssDNA attachment onto the pGlu-modified SiNPs via EDC coupling reaction. Amino-terminated ssDNA (2 μL, 1 mM), EDC (3 mg) and NHSS (0.9 mg) were added to water (30 μL) and then combined with the solution of pGlu-modified SiNPs. The mixture was held at room temperature for 12 h. Unreacted DNA was removed by centrifuging the nanoparticle solution, removing the supernatant, and resuspending nanoparticles in water. This process was repeated three times, and the DNA modified SiNPs were redispersed in phosphate buffer. The final concentration of particles was estimated to be 10 nM by UV–visible absorption. These DNA-modified SiNPs were used in the nanoparticle-enhanced SPRI measurements.

RESULTS AND DISCUSSION

Thrombin Detection with Near Infrared SPR Phase Imaging. In a first set of experiments, we demonstrate the use of near-infrared SPR-PI measurements to detect the bioaffinity adsorption of thrombin onto DNA aptamer microarrays. A schematic diagram of the SPR-PI instrument is shown in Figure 1a, and the apparatus is described in more detail in the Experimental Considerations. The important components of this measurement system are (i) an incoherent near-infrared LED light source at 860 nm (see the LED optical spectrum in Figure 1b) that was used to create phase grating images from the microarray. As observed previously,[9,10] incoherent light sources such as an LED greatly reduce the formation of interference fringes in the SPPs, which can lead to degradation of the optical image. SPPs created at 860 nm gold thin films have longer propagation distances and sharper resonances as compared to SPPs at 633 nm; we have noted the benefits of NIR excitation of SPPs previously in our SPR imaging measurements.[16] (ii) Four-element microarray chips that consisted of four gold thin film strips (1 mm × 10 mm; 45 nm gold thickness) on an SF10 substrate. Each microarray element was modified with a ssDNA sequence. The target ssDNA aptamer sequences were attached to the surface using a amino-modified T_{15} ssDNA oligonucleotide spacer sequence and a covalent pGlu attachment chemistry that has been described previously.[14] All of the DNA sequences used in these experiments are listed in Table 1. (iii) A 20 μL flow cell (shown schematically in Figure 1c) that was used to expose the DNA microarray to thrombin target solutions. The channels in the flow cell were aligned with the four microarray elements, and the flow rate was adjusted to approximately 4 μL/second to maintain a total cell residence times of about 5 s. A total target solution volume of 500 μL was continuously circulated over the DNA microarray during the experiment.

Changes in the phase shift of the reflected light from the microarray create simultaneous real-time phase shift curves for each of the microarray elements. These phase shift time curves were obtained by continuously recording sets of 60 CCD images collected at 50 ms intervals that were averaged to create a series of 3 s interval images. An example of two averaged CCD images that were obtained during a typical bioaffinity adsorption experiment are shown in Figure 2.

A postprocessing program converted these images into four time curves of phase shift ($\Delta\phi(t)$) as a function of time. These phase shift time curves of adsorption kinetics could be fit by the equation:[5]

$$\Delta\phi(t) = \Delta\phi_{eq}(1 - \exp(-\gamma t)) \quad (1)$$

where $\Delta\phi_{eq}$ is the equilibrium phase shift change and γ is the adsorption time constant. For the thrombin adsorption measurements, $\gamma = k_a C + k_d$, where k_a and k_d are the Langmuir adsorption and desorption rate constants, and C is the solution thrombin concentration. The equilibrium phase shift change $\Delta\phi_{eq}$ is proportional to the equilibrium fractional surface coverage of thrombin on the surface, θ_{eq}:

$$\Delta\phi_{eq} = S_{phase}\theta_{eq} \quad (2)$$

$$\theta_{eq} = K_{ads}C/(1 + K_{ads}C) \quad (3)$$

dx.doi.org/10.1021/ac202863k | Anal. Chem. 2012, 84, 440–445

where S_{phase} is the sensitivity (units of degrees) and K_{ads} is the Langmuir adsorption coefficient $K_{ads} = k_a/k_d$.[17] Equation 3 is, of course, the Langmuir adsorption isotherm. Often when comparing a series of measurements where γ is the same, we do not need to fit the time curves but just measure the value of $\Delta\phi(t)$ at a large fixed time as $\Delta\phi$ approaches $\Delta\phi_{eq}$.

To detect thrombin at various target solution concentrations with SPR-PI bioaffinity adsorption measurements, a four component DNA microarray was fabricated. One element of the microarray contained the ssDNA thrombin aptamer sequence A1, and a second element contained a second ssDNA thrombin aptamer sequence A2 (See Table 1 for the sequences). The other two microarray elements both contained the ssDNA control sequence Control-1 in order to detect any background effects or nonspecific adsorption. A1 is 15 mer that binds to exosite I of thrombin (fibrinogen binding site) and has been used previously in other surface surface bioaffinity sensing measurements.[18] Aptamer A2 is a 29 base ssDNA oligonucleotide that binds to exosite II of thrombin (a heparin-binding aptamer).[4,19] These two aptamers have also been used previously in aptamer assays for thrombin.[20,21]

Figure 3 shows the real-time SPR-PI measurements of adsorption kinetics that were obtained upon exposure of the

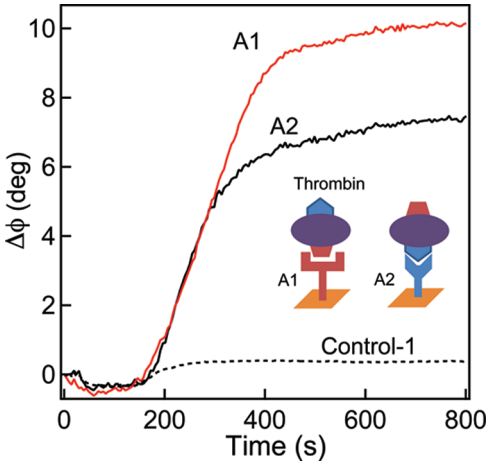

Figure 3. Real-time SPR-PI kinetic curves of the adsorption of 10 nM thrombin solution onto aptamer A1 and A2 microarray elements.

DNA microarray to a 10 nM thrombin target solution. Significant phase shifts were observed for the A1 and A2 microarray elements, and only a very small amount of phase shift was observed for the control microarray element Control-1. For the A1 and A2 microarray elements, $\Delta\phi_{eq}$ was determined to be 10.1° and 7.1°, respectively (both numbers are averages of multiple measurements with standard deviations of ±0.1°).

The differences in phase shifts that were observed upon thrombin binding to the two microarray elements A1 and A2 are attributed to the different binding affinities of A1 and A2 toward bovine thrombin. The Langmuir adsorption coefficients for these two surfaces, K_{A1} and K_{A2}, were determined from equilibrium SPRI measurements at various concentrations to be $K_{A1} = (4.4 \pm 0.4) \times 10^8\ M^{-1}$ and $K_{A2} = (1.2 \pm 0.4) \times 10^8\ M^{-1}$, respectively. The SPRI data and Langmuir fits to determine these values are shown in the Supporting Information. Using these adsorption coefficients and eq 3, at a thrombin solution concentration of 10 nM, we expect that the equilibrium relative surface coverage of thrombin on the A1 and A2 microarray elements should be $\theta_{eq} = 0.81$ and $\theta_{eq} = 0.55$, respectively. Using eq 2, these values result in a sensitivity $S_{phase} = 12.8 \pm 0.5$ deg for the thrombin SPR-PI measurements.

The results from a series of SPR-PI measurements at thrombin concentrations varying from 1.0 nM down to 100 pM are shown in Figure 4. This figure plots $\Delta\phi(t = 3000\ s)$ versus

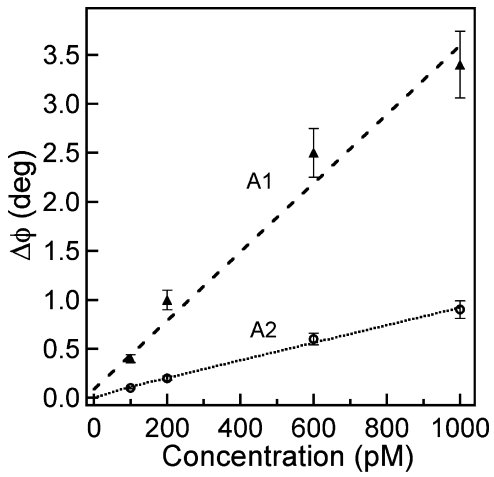

Figure 4. Quantitative SPR-PI measurements of the phase shifts($\Delta\phi$) obtained after 3000 s from A1 and A2 microarray elements for various thrombin concentrations from 1 nM to 100 pM. The ratio of the slopes of the dotted lines is 3.6 and matches with the ratio of the Langmuir adsorption coefficients for the two thrombin aptamers.

concentration; at these low concentrations, the adsorption kinetics includes contributions from diffusion to the interface,[22] so that instead of fitting the data to eq 1, we just report $\Delta\phi(3000)$ and assume that after this very long time $\Delta\phi$ will be only slightly smaller than $\Delta\phi_{eq}$. From our previous experiments, the lowest thrombin concentration that we can measure with standard SPR imaging measurements of thrombin binding onto aptamer A2 microarray elements is approximately 2.0 nM (data not shown). At a 1 nM thrombin target solution, we measure a significant $\Delta\phi(3000)$ of 3.5° ± 0.1°, which is close to the calculated $\Delta\phi_{eq}$ value of 4.0°($\Delta\phi_{eq} = S_{phase} \times \theta_{eq} = 12.8 \times 0.31$).

The lowest thrombin concentration that we observed was 100 pM, for which an equilibrium phase shift of 0.4 ± 0.05 deg was measured. For target concentrations in the picomolar range, the Langmuir adsorption isotherm is linear ($\theta_{eq} = K_{ads}C$). Therefore, the data in Figure 4 for $\Delta\phi(3000)$ as a function of thrombin concentration can be fit with straight lines with slopes of 3.6 and 1.0 degrees/nM for the A1 and A2 microarray elements, respectively ($r > 0.97$ for both of two least-squares fits). The ratio of the two slopes is 3.6, which matches very well with the ratio of the Langmuir adsorption coefficients ($K_{A1}/K_{A2} = 3.7$). A thrombin concentration of 100 pM corresponds to a fractional surface coverage of approximately 4×10^{-2}. Since the limit of detection (LOD) for standard SPRI measurements of thrombin adsorption is approximately 2.0 nM, a 100 pM LOD corresponds to a 20-fold improvement for the direct detection of thrombin with SPR-PI as compared to SPRI.

Ultrasensitive ssDNA Detection with Nanoparticle-Enhanced SPR Phase Imaging. In addition to demonstrating the enhanced sensitivity of SPR-PI versus SPRI for the direct detection of bioaffinity adsorption processes, in a second

dx.doi.org/10.1021/ac202863k | Anal. Chem. 2012, 84, 440–445

set of experiments we show that DNA-modified SiNPs can be used for "nanoparticle-enhanced SPR-PI". These nanoparticle-enhanced SPR-PI measurements exhibit a greater sensitivity as compared to previously employed "nanoparticle-enhanced SPRI"[23,24] measurements for the ultrasensitive detection of ssDNA. In the original nanoparticle-enhanced SPRI measurements, reflectivity changes observed from the bioaffinity adsorption of target ssDNA onto gold thin films is greatly enhanced by using DNA-modified nanoparticles[25,26] in the three-sequence surface hybridization scheme shown schematically in the inset of Figure 5. These experiments utilized DNA-

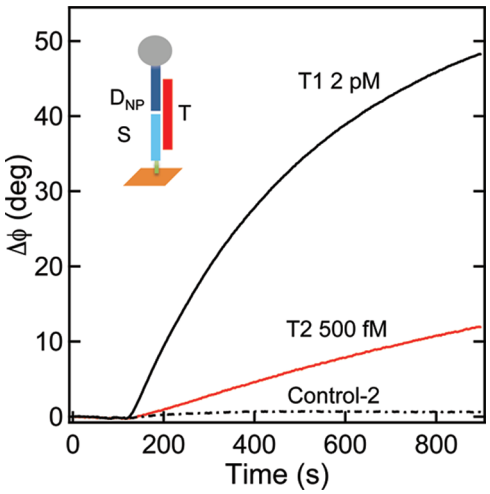

Figure 5. Real-time phase shift measurements of nanoparticle-enhanced SPR-PI. Schematic representation of the three-sequence hybridization scheme for detecting the ssDNA target sequence T (insert). The microarray elements modified with sequences S1 or S2 were exposed to a target solution of T1 (2 pM) and T2 (500 fM). The microarray was then exposed to a 1 nM solution of D_{NP}-modified SiNPs, and the real-time adsorption phase shift was recorded.

modified 13 nm gold nanoparticles (AuNPs), but subsequent papers have shown that similar sensitivity enhancement can be achieved with either polymer[27] or silica nanoparticles (SiNPs).[15] For example, we have recently used DNA-modified 120 nm SiNPs to enzymatically capture and then detect microRNA at concentrations as low as 500 fM with standard SPRI measurements.[15] In "nanoparticle-enhanced SPR-PI", SiNPs are used in the same three-sequence hybridization scheme to enhance the phase shifts observed from target ssDNA solutions at femtomolar concentrations.

We have chosen to use DNA-modified SiNPs with an average diameter of 120 nm to enhance the phase shift images in our SPR-PI measurements. When used in conjunction with the phase shift measurements, SiNPs have the advantage of possessing only a real refractive index (no absorption) in the visible and NIR spectral regions, so that the amount of phase shift enhancement provided by the SiNPs is independent of wavelength and should simply scale with the volume of the nanoparticle. The use of SiNPs to enhance the phase shift images also avoids any of the potential complications recently observed with AuNPs due to the coupling of the local plasmonic fields of the AuNP with the gold thin film surface.[28,29]

Figure 5 plots the real-time SPR-PI kinetic curves for the simultaneous detection of multiple target ssDNA with nanoparticle-enhanced SPR-PI. A DNA microarray that consisted of two probe sequence elements (S1 and S2) and a control sequence element (Control-2) was used (refer to Table 1 for the sequences). This microarray was first exposed for 3 h to a target solution (500 μL total volume) containing the two ssDNA sequences T1 and T2 at concentrations of 2 pM and 500 fM, respectively. The two ssDNA sequences specifically adsorbed from this target solution onto their respective cDNA microarray elements S1 and S2. After 3 h, the target solution was then replaced with a 1 nM solution of DNA-modified SiNPs, and the SPR-PI kinetics curves in Figure 5 were recorded. Very large phase shift changes were observed for the two probe microarray elements and are attributed to the formation of the three-sequence nanoparticle/DNA surface complex that is depicted in the inset of Figure 5. The SPR-PI kinetic curve for the ssDNA control sequence (Control-2) microarray element is also shown in Figure 5; only a very small amount of phase shift (1° or less after 900 s) was observed. This small phase shift is attributed to differences of the refractive index of the two bulk solutions and was subtracted from the real-time kinetics curves of the two probe elements to yield values of $\Delta\phi(t = 900\ \text{s})$ of 48.4° for element S1 and 11.9° for element S2, respectively. Note that SiNP adsorption from the 1 nM solution is approaching its limiting value ($\Delta\phi_{eq}$) at 900 s; this is because we are monitoring the adsorption of the SiNPs from a 1 nM solution, not the adsorption of target ssDNA from picomolar or femtomolar solutions which can take hours to reach equilibrium.[17]

The very large phase shifts observed from the nanoparticle-enhanced SPRI measurements for detecting ssDNA at 2 pM and 500 fM suggest that even lower ssDNA concentrations should be measurable. Figure 6 plots a series of real-time kinetic

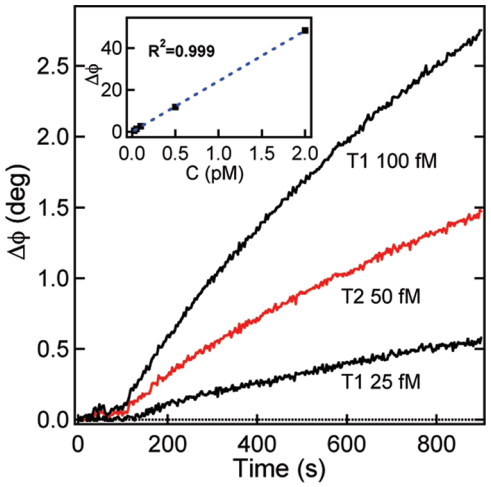

Figure 6. Real-time SPRI kinetic curve for the multiplexed detection of femtomolar concentration of target DNA (T1 of 25 fM, T2 of 50 fM and T1 of 100 fM) with nanoparticle-enhanced SPR-PI measurements. The inset shows the linear behavior of the phase shift for low concentrations.

curves for the adsorption of DNA-modified SiNPs onto DNA microarrays that have been exposed to target solutions that contained ssDNA at concentrations ranging from 100 to 25 fM. Even at 25 fM, a phase shift $\Delta\phi(900)$ of 0.5° was at a S/N ratio greater than 5. The inset of the figure plots the $\Delta\phi(900)$ observed in the SPR-PI versus DNA target concentration; a linear slope was observed over the entire concentration range 25 fM to 2 pM. We report a conservative value of 25 fM as a

dx.doi.org/10.1021/ac202863k | Anal. Chem. 2012, 84, 440−445

LOD for nanoparticle SPR-PI; this value is 20 times lower than the 500 fM LOD observed in SPRI. The 20× enhancement observed in the nanoparticle-enhanced SPR-PI measurements value exactly matches the 20× improvement in sensitivity observed in the direct SPR-PI thrombin detection measurements.

CONCLUSIONS

In this paper, we have demonstrated that near-infrared SPR-PI measurements can be used to significantly improve the sensitivity of microarray SPR imaging biosensing measurements. Specifically, we have demonstrated that the multiplexed bioaffinity adsorption kinetic curves obtained from SPR phase images of DNA aptamer microarrays can be used to detect the protein thrombin at concentrations as low as 100 pM. This detection limit is approximately 20 times more sensitive than our previously reported SPRI measurements and corresponds to the detection of a fractional equilibrium surface coverage of approximately $\theta_{eq} = 10^{-2}$ for the 36 kDa protein. In a second set of experiments, we also demonstrated that it is possible to employ DNA-modified SiNPs to greatly enhance the sensitivity of the phase shift images in SPR-PI; this "nanoparticle-enhanced SPR-PI" was used to simultaneously detect two 38mer ssDNA target oligonucleotides at concentrations as low as 25 fM. This detection limit corresponds to the detection of a fractional surface coverage of approximately $\theta_{eq} = 10^{-6}$. The SPR-PI measurements described in this paper are not limited to only DNA microarrays but should also be immediately applicable to bioaffinity measurements using protein, peptide, and carbohydrate microarrays. Similarly, the DNA-modified SiNPs used in nanoparticle-enhanced SPR-PI measurements can be replaced with other protein-modified or carbohydrate-modified nanoparticles for various ultrasensitive biosensing applications. In the immediate future, we will improve our near-infrared SPR-PI instrumental apparatus in order to accommodate a larger number of microarray elements and incorporate our surface enzyme chemistries into the nanoparticle-enhanced SPR-PI measurements for additional biosensing selectivity and sensitivity.

ASSOCIATED CONTENT

Supporting Information

Additional information as noted in text. This material is available free of charge via the Internet at http://pubs.acs.org.

AUTHOR INFORMATION

Corresponding Author

*E-mail: rcorn@uci.edu.

ACKNOWLEDGMENTS

This research was supported by the National Science Foundation (Grant CHE-0551935). We thank Kohei Nakamoto for providing the TOC graphic.

REFERENCES

(1) Stears, R. L.; Martinsky, T.; Schena, M. *Nat. Med.* **2003**, *9*, 140.
(2) van Hal, N. L. W.; Vorst, O.; van Houwelingen, A.; Kok, E. J.; Peijnenburg, A.; Aharoni, A.; van Tunen, A. J.; Keijer, J. *J. Biotechnol.* **2000**, *78*, 271.
(3) He, P.; Shen, L.; Cao, Y.; Lia, D. *Anal. Chem.* **2007**, *79*, 8024.
(4) Li, Y.; Lee, H. J.; Corn, R. M. *Anal. Chem.* **2007**, *79*, 1082.
(5) Wegner, G. J.; Wark, A. W.; Lee, H. J.; Codner, E.; Saeki, T.; Fang, S.; Corn, R. M. *Anal. Chem.* **2004**, *76*, 5677.
(6) Chandra, H.; Srivastava, S. *Proteomics* **2010**, *10*, 717.
(7) Smith, E. A.; Thomas, W. D.; Kiessling, L. L.; Corn, R. M. *J. Am. Chem. Soc.* **2003**, *125*, 6140−6148.
(8) Lee, H. J.; Li, Y.; Wark, A. W.; Corn, R. M. *Anal. Chem.* **2005**, *77*, 5096.
(9) Halpern, A. R.; Chen, Y.; Corn, R. M.; Kim, D. *Anal. Chem.* **2011**, *83*, 2801.
(10) Kabashin, A. V.; Patskovsky, S.; Grigorenko, A. N. *Opt. Express* **2009**, *17* (23), 21191.
(11) Patskovsky, S.; Jacquemart, R.; Meunier, M.; De Crescenzo, G.; Kabashin, A. V. *Sens. Actuators, B: Chem* **2008**, *133*, 628.
(12) Wong, C. L.; Ho, H. P.; Suen, Y. K.; Kong, S. K.; Chen, Q. L.; Yuan, W.; Wu, S. Y. *Biosens. Bioelectron.* **2008**, *24*, 606.
(13) Yu, X. L.; Ding, X.; Liu, F. F.; Wei, X.; Wang, D. X. *Meas. Sci. Technol.* **2008**, *19*, 015301.
(14) Chen, Y. L.; Nguyen, A.; Niu, L. F.; Corn, R. M. *Langmuir* **2009**, *25*, 5054.
(15) Zhou, W.-J.; Chen, Y.; Corn, R. M. *Anal. Chem.* **2011**, *83*, 3897.
(16) Nelson, B. P.; Frutos, A. G.; Brockman, J. M.; Corn, R. M. *Anal. Chem.* **1999**, *71*, 3928.
(17) Lee, H. J.; Wark, A. W.; Corn, R. M. *Langmuir* **2006**, *22*, 5241.
(18) Bock, L. C.; Griffin, L. C.; Latham, J. A.; Vermaas, E. H.; Toole, J. J. *Nature* **1992**, *355*, 564.
(19) Tasset, D. M.; Kubik, M. F.; Steiner, W. *J. Mol. Biol.* **1997**, *272*, 688.
(20) Edwards, K. A.; Baeumner, A. J. *Anal. Bioanal. Chem* **2010**, *398*, 2635.
(21) Fredriksson, S.; Gullberg, M.; Jarvius, J.; Olsson, C.; Pietras, K.; Gustafsdottir, S. M.; Ostman, A.; Landegren, U. *Nat. Biotechnol.* **2002**, *20*, 473.
(22) Bourdillon, C.; Demaille, C.; Moiroux, J.; Saveant, J. M. *J. Am. Chem. Soc.* **1999**, *121*, 2401.
(23) Gifford, L. K.; Sendroiu, I. E.; Corn, R. M.; Luptak, A. *J. Am. Chem. Soc.* **2010**, *132*, 9265.
(24) Li, Y.; Wark, A. W.; Lee, H. J.; Corn, R. M. *Anal. Chem.* **2006**, *78*, 3158.
(25) He, L.; Musick, M. D.; Nicewarner, S. R.; Salinas, F. G.; Benkovic, S. J.; Natan, M. J.; Keating, C. D. *J. Am. Chem. Soc.* **2000**, *122*, 9071.
(26) Sendroiu, I. E.; Gifford, L. K.; Luptak, A.; Corn, R. M. *J. Am. Chem. Soc.* **2011**, *133*, 4271.
(27) Ortega-Vinuesa, J. L.; Hidalgo-Alvarez, R.; de las Nieves, F. J.; Davey, C. L.; Newman, D. J.; Price, C. P. *J. Colloid Interface Sci.* **1998**, *204*, 300.
(28) Hutter, E.; Fendler, J.; Roy, D. *J. Phys. Chem. B* **2001**, *105*, 11159.
(29) Peterlinz, K. A.; Georgiadis, R. *Langmuir* **1996**, *12*, 4731.